

Response Controlling of Corner Lateral Displacements of Structures due to Time-Varying Torsion by using MR Damper

Kambiz Takin¹, Behrokh H. Hashemi^{2*} and Masoud Nekooei¹

¹Department of Civil Engineering, Science and Research Branch, Islamic Azad University, Tehran, Iran; omran@engineer.com, msnekooei@gmail.com

²Structural Engineering Research Center (SERC), International Institute of Earthquake Engineering and Seismology (IIEES), Tehran, Iran; behrokh_h_h@yahoo.com

Abstract

This article is all about the combination of an intelligent system such as a photoelectric sensor with MR damper that would be able to control the shear and torsional displacements of buildings. This paper will show how the appropriate algorithm is for current injection into MR Damper in order to control the lateral displacement of structure when the eccentricity of the load and damping forces are changing. In this article by using the CQC, DSC, Vanmark, Humar, Gupta and exact methods the lateral forces, torsional moments, shear stresses and current in MR damper obtained for one storey building with external bracing system. The application of this study is for critical structures such as power plants, military and governmental buildings construction, nuclear power plants, etc. The torsional modes can be very destructive, unpredictable and cannot be calculated with common software so, an exact-method is also utilized.

Keywords: Dynamic Analysis, Eccentricity, Exact Method, Lateral Displacement, MR Damper, Torsion

1. Introduction

Semi-active control systems can provide reliability for passive systems and require low power supply than active control systems. Lower power supply and higher reliability make the semi-active control systems a reliable system for buildings. The MR dampers look like a viscous damper, but inside of the MR damper is filled with a particular fluid, which contains small polarizable ingredients. The fluid inside the damper can be transitioned from liquid to solid by variation of the magnetic field, which produced by the copper coil surrounding the piston. When the injected current is none, this damper behaves as a viscous damper and when the current is injected through the copper coil, the fluid inside a damper becomes semi-solid. The yield strength of this liquid depends on the applied current¹⁻⁴. The main characteristic of this fluid is the capability of changing phase from free flowing to semi-solids. They

are able to generate large forces with highly reliability by a modest cost, and very low power. So many researchers spend extensive research on MR dampers since 1992. The main results of analytical and experimental studies have showed that these dampers are very reliable devices in applications^{5,6}. For the first time, Large-scale MR damper has been presented at the University of Notre Dame and in 2002 transferred to the University of Illinois. They showed that these semi-active control system in large-scale are capable of providing the considerable resisting forces¹⁻⁵. In general a structure collapse when one of its vital members fails causing the failure and damage of adjoining elements¹⁴. It is well recognized that current seismic design codes are based on elastic behavior and account for the inelastic behavior indirectly. It has been noted that large inelastic deformation in a pretty unpredictable behavior will happen for structure designed by such procedures under sever earthquake^{15,16}.

*Author for correspondence

The different kinds of semi-active control devices were, including dampers with variable orifice, variable friction, and dampers with controllable fluid. These systems have more attractive because they operate by low power and very reliable. The semi-active control system is defined as a device, which has constant mechanical energy but the dynamic properties can be varied. This device is adaptable and expected to be effective for building response reduction. Therefore, the semi-active systems do not require huge power unlike, active control systems. In addition, these systems are inherently stable, which result in suitable performances for structural response⁴⁻⁶. The possibility of using the MR damper as a vibrational control system performed by different controller algorithm in a structure and many researchers have studied the response of structures with MR dampers². Most of these studies included small-scale MR dampers that could not be applicable to real size of structures. Spencer et al., performed comprehensive investigation about MR dampers and developed their investigation based on Bouc-Wen hysteresis model. This model was used for demonstrate the performance of MR dampers¹¹⁻¹². After that, Dyke, et al.¹¹ developed their model by using a MR damper to control a multi-storey building¹ and a large-scale 20-ton MR damper is being tested at the University of Notre Dame⁷. The performance of neural networks and adaptive Systems of neuro-fuzzy inference in simulating the inverse dynamic behavior of MR dampers has investigated by Ghasemi⁹. The behavior of a MR damper is placed in the structure between the first storey and ground for controlling the seismic response has investigated by Mousaad¹⁰. The effects of yield mechanism selection on the performance based plastic design of steel moment frame.

2. The Mass and Stiffness Matrices

The mass and stiffness matrices can be obtained based on the center of mass or stiffness. The easiest method is to consider the center of mass for calculation. Therefore, the mass and stiffness matrices in Torsion-Shear Single-Storey structure are being calculated by taking the degrees of freedom at the center of mass. The mass matrix remains diagonal and the stiffness matrix determines based on the eccentricity. An intermediate moment frame system with a rigid roof has been considered and the center of mass and center of rigidity were identified as C.M. and C.R. The transitional and torsional degrees of freedom considered at the center of mass. Where, e_x and e_y are the eccentricity

of load in x and y directions. Therefore, the stiffness and mass matrices are obtained from Equations (1–2). These matrices are obtained from Equations (3–4) for two story buildings and can be expanded for n-storey building⁸.

$$[K] = \begin{bmatrix} K_x & 0 & -K_x e_y \\ 0 & K_y & K_y e_x \\ -K_x e_y & K_y e_x & K_\theta + K_x e_y^2 + K_y e_x^2 \end{bmatrix} \quad (1)$$

$$[M] = \begin{bmatrix} m_x & 0 & 0 \\ 0 & m_y & 0 \\ 0 & 0 & m_\theta \end{bmatrix} \quad (2)$$

$$[K] = \begin{bmatrix} K_{x1} + K_{x2} & 0 & -K_{x1}e_{y1} - K_{x2}e_{y12} & -K_{x2} & 0 & K_{x2}e_{y2} \\ 0 & K_{y1} + K_{y2} & K_{y1}e_{x1} + K_{y2}e_{x12} & 0 & -K_{y2} & -K_{y2}e_{x2} \\ & & K_{\theta 1} + K_{x1}e_{y1}^2 & & & -(K_{\theta 2} + K_{x2}e_{y2}^2) \\ -K_{x1}e_{y1} & K_{y1}e_{x1} & + K_{y1}e_{x1}^2 + K_{\theta 2} & K_{x2}e_{y12} & -K_{y2}e_{x12} & + K_{y2}e_{x2}^2 + K_{x2}e_{y2}\Delta y \\ -K_{x2}e_{y12} & + K_{y2}e_{x12} & + K_{x2}e_{y12}^2 + K_{y2}e_{x12}^2 & & & + K_{y2}e_{x2}\Delta x \\ -K_{x2} & 0 & K_{x2}e_{y12} & K_{x2} & 0 & -K_{x2}e_{y2} \\ 0 & -K_{y2} & -K_{y2}e_{x12} & 0 & K_{y2} & K_{y2}e_{x2} \\ & & -(K_{\theta 2} + K_{x2}e_{y2}^2) & & & K_{\theta 2} + K_{x2}e_{y2}^2 \\ K_{x2}e_{y2} & -K_{y2}e_{x2} & + K_{y2}e_{x2}^2 + K_{x2}e_{y2}\Delta y & -K_{x2}e_{y2} & K_{y2}e_{x2} & + K_{y2}e_{x2}^2 \\ & & + K_{y2}e_{x2}\Delta x & & & \end{bmatrix} \quad (3)$$

$$[M] = \begin{bmatrix} m_{x1} & 0 & 0 & 0 & 0 & 0 \\ 0 & m_{y1} & 0 & 0 & 0 & 0 \\ 0 & 0 & m_{\theta 1} & 0 & 0 & 0 \\ 0 & 0 & 0 & m_{x2} & 0 & 0 \\ 0 & 0 & 0 & 0 & m_{y2} & 0 \\ 0 & 0 & 0 & 0 & 0 & m_{\theta 2} \end{bmatrix} \quad (4)$$

3. Numerical Example

The size of desired one-storey building along x and y axis is 35 by 35 meters and Coalinga earthquake record considered for this study. The transitional and rotational stiffness along x and y axis are 270t/m and is 108000t.m. The total mass of each floor is 635t and rotational mass is 17500t.m². The mass and stiffness matrices obtain as Equations (5–6).

$$[K] = \begin{bmatrix} K_x & 0 & -K_x e_y \\ 0 & K_y & -K_y e_x \\ -K_x e_y & -K_y e_x & K_\theta + K_x e_y^2 + K_y e_x^2 \end{bmatrix}$$

$$\Rightarrow [K] = \begin{bmatrix} 2750 & 0 & -2750e_y \\ 0 & 2750 & -2750e_x \\ -2750e_y & -2750e_x & 108000 + 2750e_y^2 + 2750e_x^2 \end{bmatrix} \quad (5)$$

$$[M] = \begin{bmatrix} M_x & 0 & 0 \\ 0 & M_y & 0 \\ 0 & 0 & J \end{bmatrix} = \begin{bmatrix} 635 & 0 & 0 \\ 0 & 635 & 0 \\ 0 & 0 & 17500 \end{bmatrix} \quad (6)$$

The approximate structural model considered with external braces at the corners of the structure that equipped with MR Dampers shown at Figure 1, which has ability to control the lateral displacements caused by structural torsional and transitional modes. The objective is to determine the lateral displacement limit that active the input electric current to this damper system. The purpose is to prevent activation of MR Damper while the structure is experiencing low lateral displacements due to low speed wind, low earthquake forces, and vibrations during operation. In fact, when the displacement in damper is under the predefine range, the damper acts like a conventional viscous damper. Figure 4. shows the general view of a structure with location of dampers.

3.1 The Lateral Forces and Torsional Moments due to an Earthquake in Floors

In buildings without eccentricity, seismic forces assumed perpendicular to the main structural directions. In fact, this assumption is not correct, because the forces due to the earthquakes can imposed to the structure in any direction and the responses are varied. However, to facilitate the calculation these forces assumed in the two perpendicular directions of the structure. The torsional moments can create great changes in base shear of

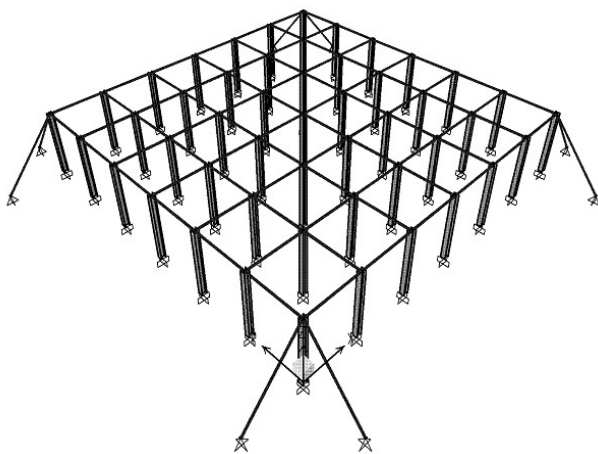


Figure 1. An overview of structure with the MR dampers can be placed at the external bracing.

structure. Figures 2 to 4 display the seismic lateral forces curves in the x, y directions and torsional moments perpendicular to eccentricity. According to these curves it can be concluded that, with increasing eccentricity the seismic lateral forces increased in the x and y directions. In all methods except exact-method, at first the created torsional moment declines, then increases and decreases again. The moment has increasing trend and results are very different with the other methods. The lateral forces in the x-direction conform at DSC and CQC methods, SRSS and ABS methods show greatest values and the exact-method has lower values, relatively. The lateral forces in the x-direction also conform at DSC and CQC methods and non-correlated methods show the greatest values. The exact-method shows greater values than other methods. The results of Humar and Vanmark methods

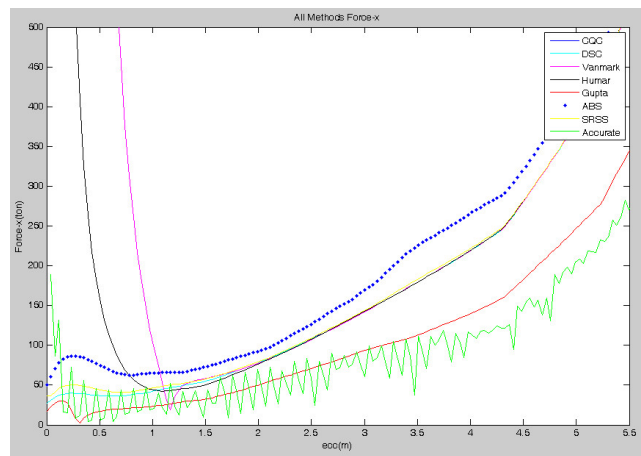


Figure 2. The relationship between eccentricity and lateral forces in the x-direction.

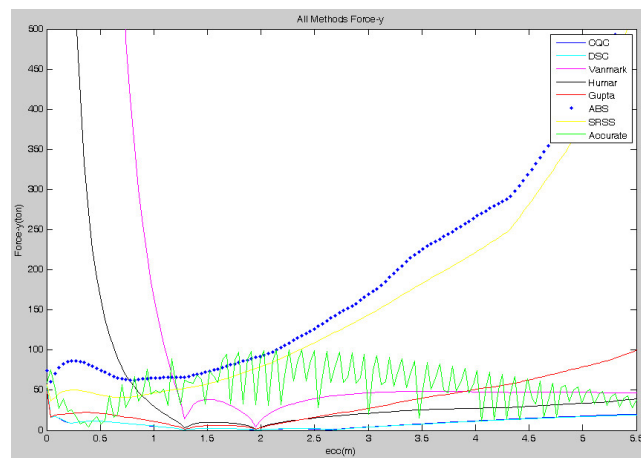


Figure 3. The relationship between eccentricity and lateral forces in the y-direction.

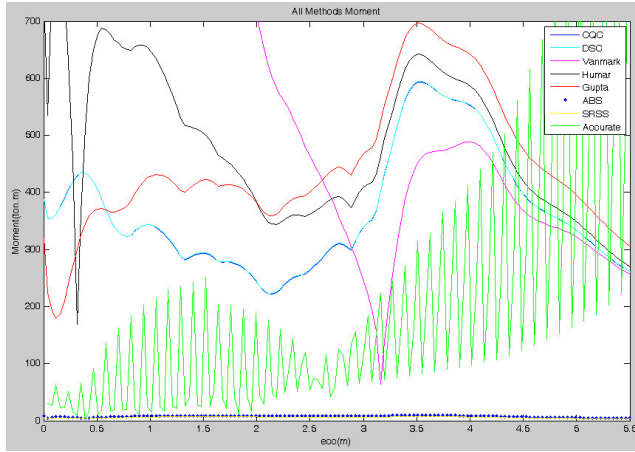


Figure 4. The relationship between eccentricity and torsional moment of floors.

are very different from the other methods and cannot be trusted for this kind of buildings. According to the obtained results for determine the lateral forces, the CQC and DSC methods can used, but to calculate the torsional moment of floors due to increasing with eccentricity, the exact-method must be considered.

3.2 The Created Forces in Dampers

Lateral forces and torsional moments caused by earthquake can transmit forces to the outer diagonal braces. These braces are equipped with semi-active MR dampers, which the purpose of placing them is to reduce displacements at the corners of structural. This system also can lead to reduce structural response in shear mode as well. These forces obtain from Equations 7–8.

$$\begin{aligned}
 F_1 + F_2 &= -F_x \\
 -F_1\left(\frac{a}{2} - e\right) + F_2\left(\frac{a}{2} + e\right) + F_x e - M &= 0 \\
 \Rightarrow \left(\frac{a}{2} - e\right)F_1 - \left(\frac{a}{2} + e\right)F_2 &= eF_x - M \\
 \Rightarrow \left\{ \begin{aligned} -\left(\frac{a}{2} - e\right)F_1 - \left(\frac{a}{2} - e\right)F_2 &= \left(\frac{a}{2} - e\right)F_x \\ \left(\frac{a}{2} - e\right)F_1 - \left(\frac{a}{2} + e\right)F_2 &= eF_x - M \end{aligned} \right\} &\Rightarrow \\
 \left\{ \begin{aligned} F_1 &= \frac{\left(-\frac{a}{2}\right)F_x - M}{a} = -\frac{F_x}{2} - \frac{M}{a} \\ F_2 &= \frac{\left(-\frac{a}{2}\right)F_x + M}{a} = -\frac{F_x}{2} + \frac{M}{a} \end{aligned} \right. &\quad (7) \\
 &\quad (8)
 \end{aligned}$$

In Figures 5 to 8, display the relationship between the lateral forces that generated by the damper and eccentricity in CQC and DSC methods for the different target displacements. In some of these curves at the lower eccentricities towards the target displacement, the damping force is none, because, the available displacements are lower than the target displacements. In x direction close to eccentricity, the semi-active system does not activate up to 1.75 meters of eccentricity, but after that the damping forces increasing exponentially. In Vanmark method, at the lower eccentricities generated forces in damper are acceptable but after that, these forces are much higher than the other methods, which are shown at Figures 9 to 10. In the other methods, the general trend remains the same, which can be seen in Figures 11 to 16.

By increasing the target displacement, the growth of damping forces has delayed from zero to maximum. For example, at the target displacement of 10 centimeters, the damper will be activated at the eccentricity of 4.4 meters by increasing the eccentricity, the damping forces will be increased significantly. According to the Figures 5 to 16 at far distance to the eccentricity in x direction, the damper is activated at the eccentricity between 1.76 to 2.41 meters and in the other scenarios, the displacement has shown lower values. The same trend can be seen in y direction with an exception, the activation of damper can be seen at the lower eccentricities in higher target displacements and in some kind of these target displacements. The damping system does not activate, because the corner lateral displacements are lower than the displacement target.

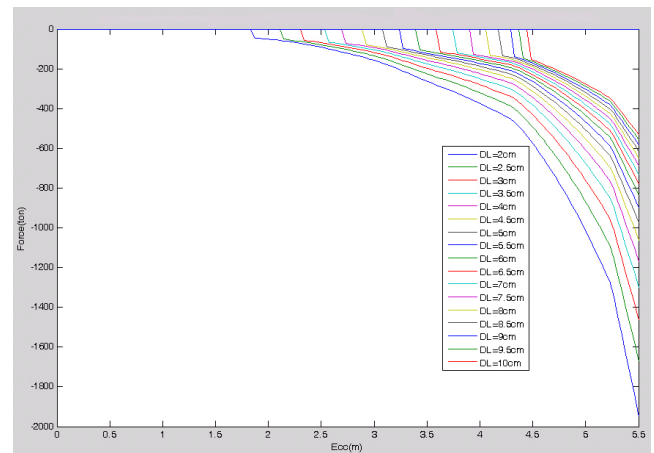


Figure 5. The relation between eccentricity and corner lateral displacement, near to eccentricity in x-direction with CQC method.

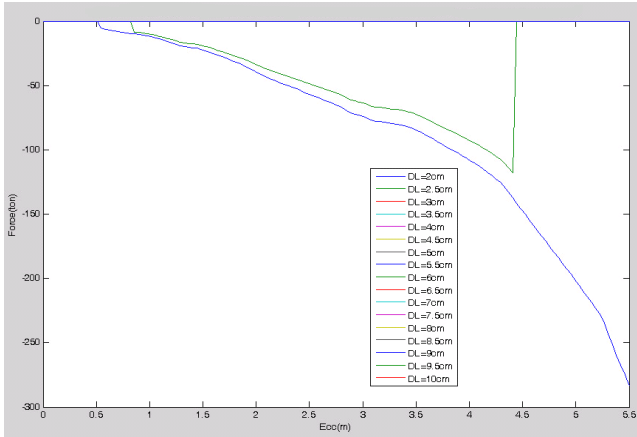


Figure 6. The relation between eccentricity and corner lateral displacement, far from eccentricity in x-direction with CQC method.

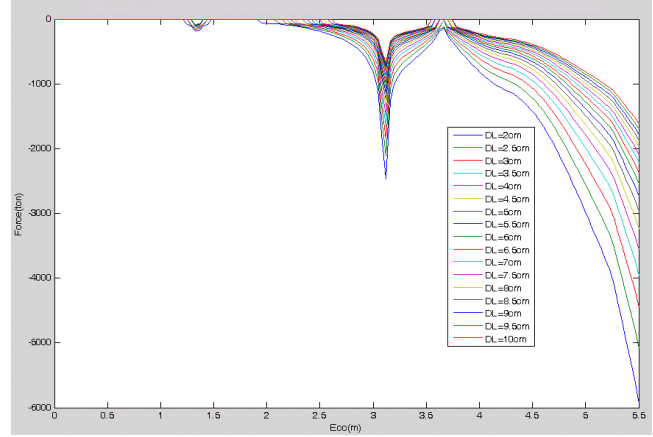


Figure 9. The relation between eccentricity and corner lateral displacement, near to eccentricity in x-direction with Vanmark method.

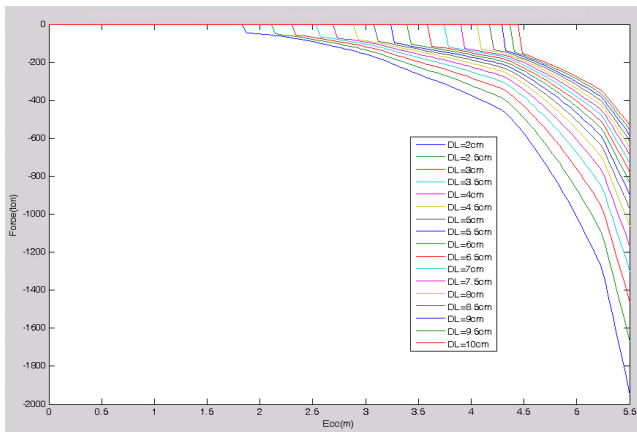


Figure 7. The relation between eccentricity and corner lateral displacement, near to eccentricity in x-direction with DSC method.

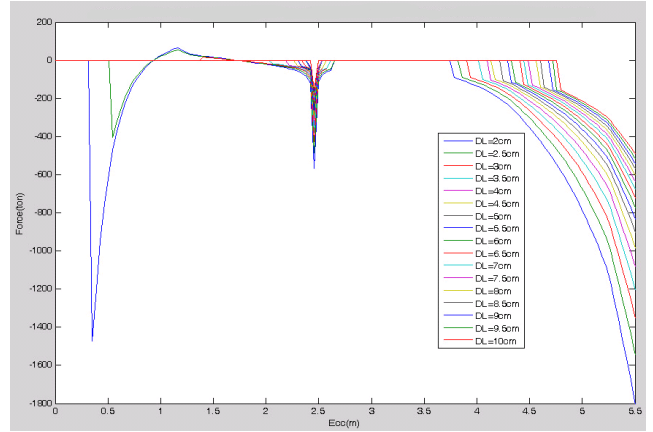


Figure 10. The relation between eccentricity and corner lateral displacement, far from eccentricity in x-direction with Vanmark method.

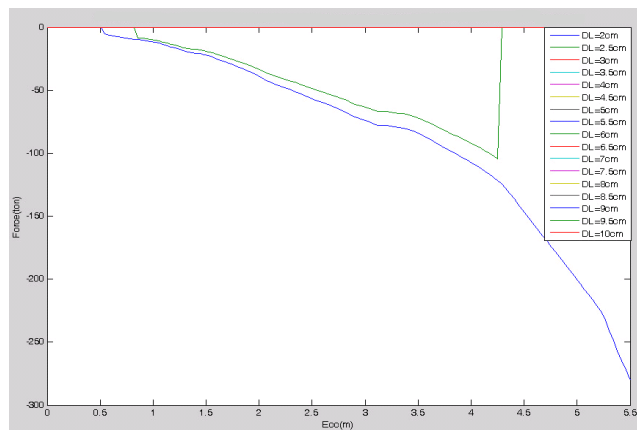


Figure 8. The relation between eccentricity and corner lateral displacement, far from eccentricity in x-direction with DSC method.

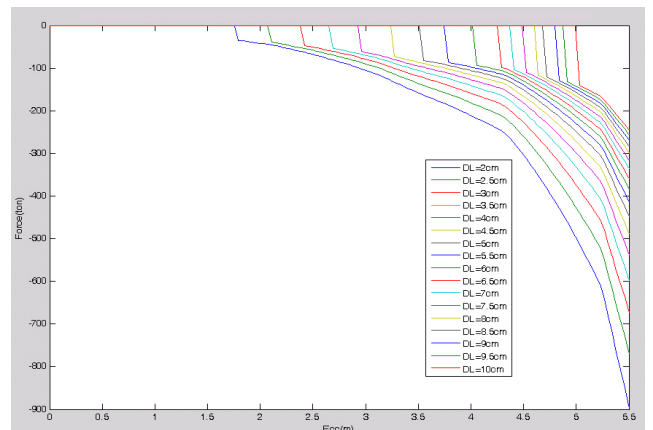


Figure 11. The relation between eccentricity and corner lateral displacement, near to eccentricity in x-direction with Gupta method.

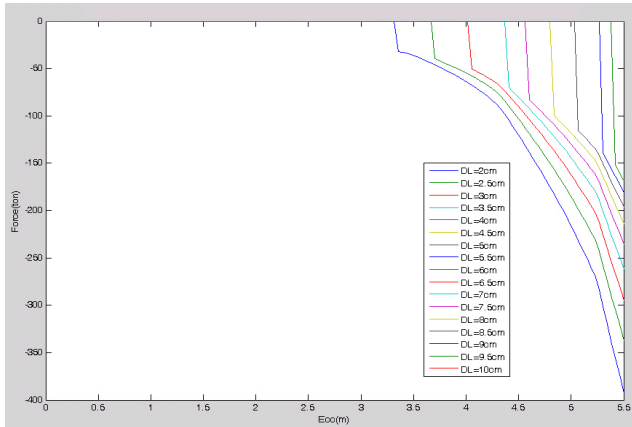


Figure 12. The relation between eccentricity and corner lateral displacement, far from eccentricity in x-direction with Gupta method.

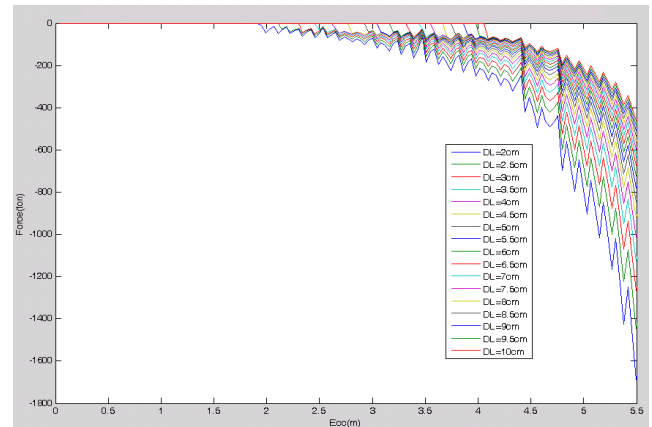


Figure 15. The relation between eccentricity and corner lateral displacement, near to eccentricity in x-direction with exact-method.

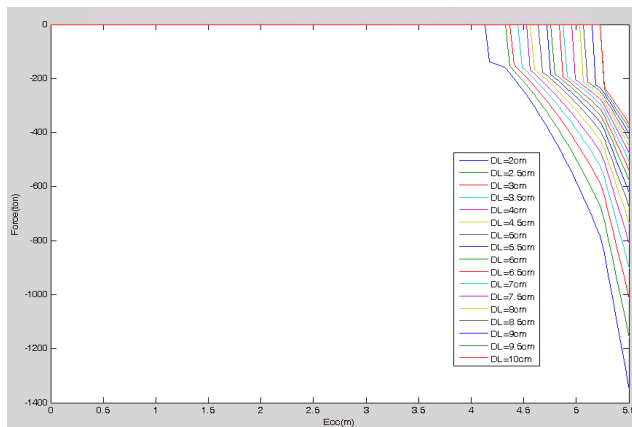


Figure 13. The relation between eccentricity and corner lateral displacement, near to eccentricity in x-direction with Humar method.

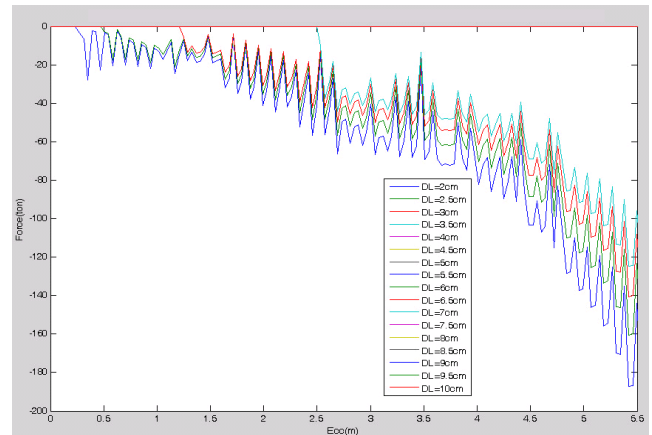


Figure 16. The relation between eccentricity and corner lateral displacement, far from eccentricity in x-direction with exact-method.

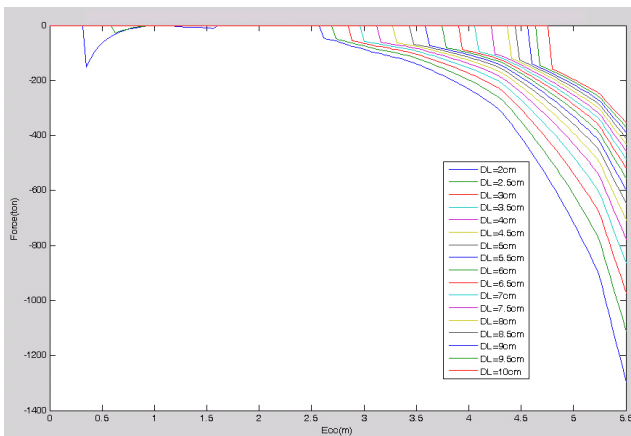


Figure 14. The relation between eccentricity and corner lateral displacement, far from eccentricity in x-direction with Humar method.

4. Bingham Plasticity Model

The Bingham plasticity model is useful in describing the field-dependent fluid characteristic. Phillips¹⁷ derived an equation, which can be obtained from the pressure gradient in the flow according to Bingham model. Gavin et al.^{3,4} represent the idea, based on the simple model based on parallel-plate and describing the relation between force and velocity of cylinder MR dampers. Other researchers^{16,18} have employed this method to investigate for MR dampers. This model was developed by Spencer et al.¹⁰. In this model, the total damper force F that contain a controllable force F_c due to controllable yield stress and F_{UC} is an uncontrollable force. The F_{UC} includes, a viscous force F_η and F_f is a constant friction force. Thus, these forces

expresses with Equations 9–13 and also demonstrates with Figure 17.

$$F_{\eta} = \left(1 + \frac{wh}{2A_p}\right) \frac{12\eta LA_p^2}{wh^3} v_0 \quad (9)$$

$$F_{\tau} = C \frac{\tau_0 LA_p}{h} \text{sgn}(v_0) \quad (10)$$

$$C = 2.07 + \frac{1}{1+0.4T} \quad \& \quad 2.04 < C < 3.07 \quad (11)$$

$$T = \frac{wh^2 \tau_0}{12A_p \eta v_0} \quad (12)$$

$$F = F_{\tau} + F_{\eta} + F_f \quad (13)$$

In these equations, A_p is the piston's cross sectional area, h is the distance between plates, L is the effective pole length, w is the width of the plate, η is the Newtonian viscosity and τ_0 is the yield stress of fluid.

In this article, the results of 20-tons MR damper considered, which in this device the length of damper is 8.4cm, air gap is 2mm, width of plate is 63.2cm, cross section area is 271cm², viscosity is 1.3Pa/sec and constant friction force is 6.34kN. Also, the maximum and minimum shear stress is 0.05 and 62kN (Tsang et al., 2006). According to the Figures (18-19) in CQC and DSC methods, with decreasing the target displacement the shear stress increases and activation of semi-active

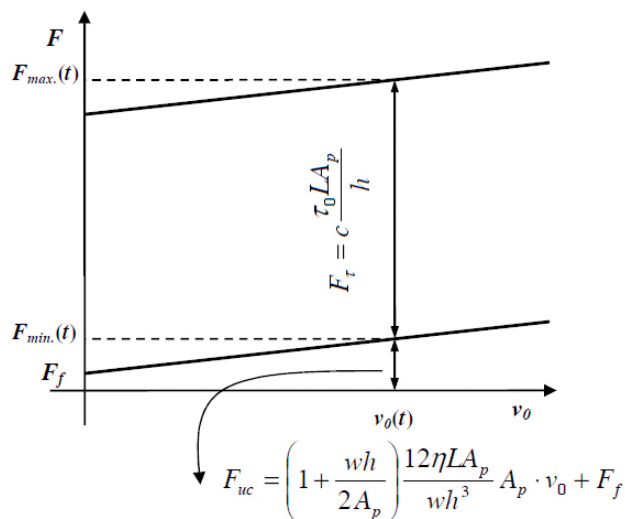


Figure 17. The relation between damper force and velocity.

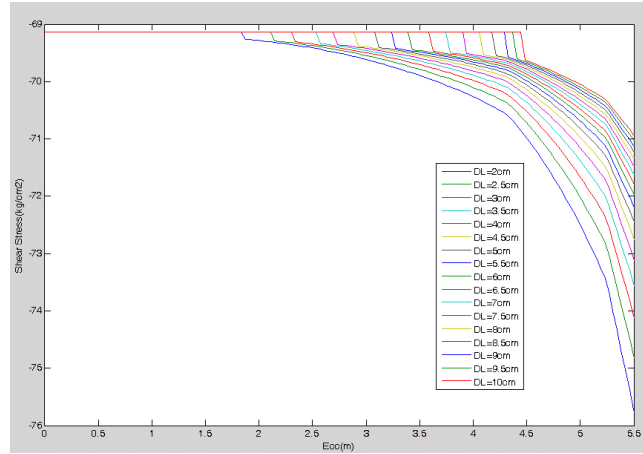


Figure 18. The relation between eccentricity and shear stress in MR damper with CQC method.

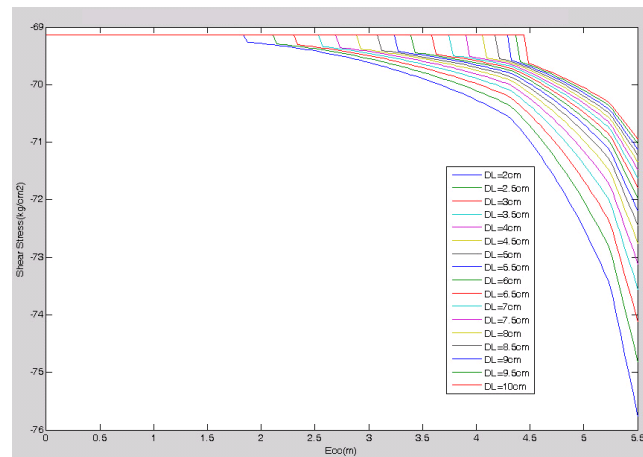


Figure 19. The relation between eccentricity and shear stress in MR damper with DSC method.

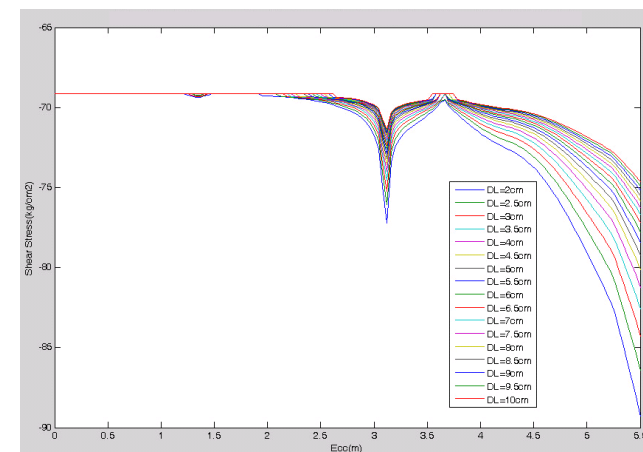


Figure 20. The relation between eccentricity and shear stress in MR damper with Vanmark method.

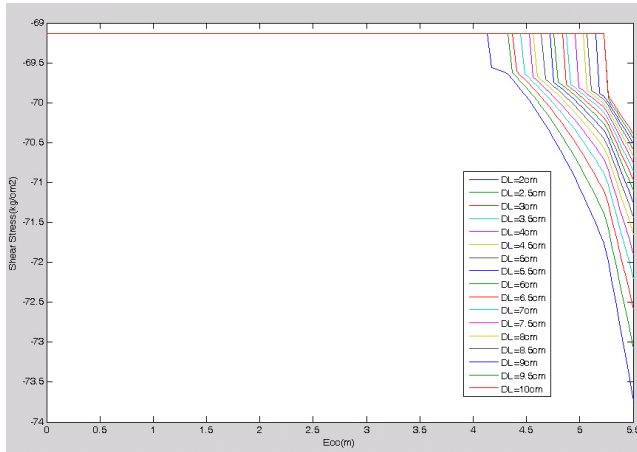


Figure 21. The relation between eccentricity and shear stress in MR damper with Humar method.

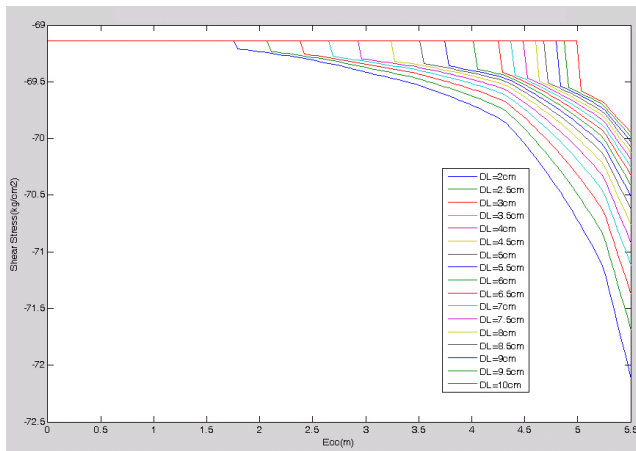


Figure 22. The relation between eccentricity and shear stress in MR damper with Gupta method.

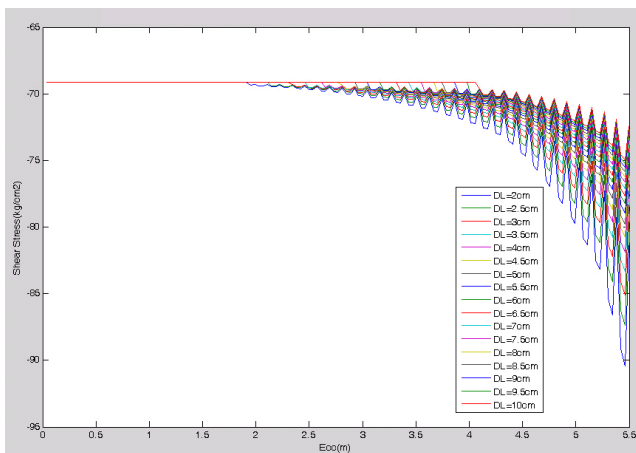


Figure 23. The relation between eccentricity and shear stress in MR damper with exact-method.

system delayed. With increasing the eccentricity for some target displacements, the damper cannot bear for this shear stresses and a stronger one must be used. Formerly, the Vanmark method shows higher values than the other methods, but the range of shear stresses are in a reasonable limit. The shear stress of Vanmark method shows different trend from the other methods. These curves show sharp rising in some parts and cannot be trusted for these kinds of buildings. The results of this method shown at Figure 20. According to Figures 21 to 22, the trend of Humar and Gupta methods similar to DSC and CQC methods, which by increasing the eccentricity and decreasing the target displacement, the trend of shear stress is ascending. In Figure 23 shows the exact-method has some oscillations, but the general trend of this method is similar to CQC and DSC methods.

5. The Relation between Eccentricity and Current in MR Damper

The curves obtained based on the displacement target and the angle between the brace and the horizontal axes for the displacement target of 4 cm. In all displacements, the rate of current will soar by increasing the eccentricity. By continuing in increasing of the eccentricity, it increase exponentially. According to Figures 24 to 27, the curve obtained by CQC and DSC methods shows that the relationship of current with eccentricity have the same trend in both methods. In this part the current, which needed for displacement control is considered. The amount of current is needed to control displacement with MR damper is completely reasonable. At first, in all methods by increasing the eccentricity the required current for controlling with MR damper has increased sharply and then exponentially. According to Figures 24 to 27, the CQC and DSC methods have same trend. As can be seen in these curves, by increasing the eccentricity and the displacement target or the angle of brace with horizontal axis, the required electric current in order to control the lateral displacement increases. According to the results, 30 Amps shows a reasonable amount to control the lateral displacement. As can be seen in Figures 28 to 29, the curves obtained in Vanmark’s method shows a different trend. After passing some zero current, it rises slightly then becomes zero, and then increases with a higher rate, then becomes zero again. At the end, by increasing

the eccentricity, shows an ascending trend. Due to a big difference in results in Vanmark and the other methods, this method is not recommended, but it shows a reasonable range of Amps required for the lateral displacement control. Humar method as can be seen at Figures 30 to 31, also shows a different trend and is not recommended for calculation. According to Figures 32 to 33, Gupta method has the same trend as the other methods and can be used to determine the Amps input range required for MR Damper. The trends in Mode-Displacement method is very similar to CQC and DSC, but the amps values in the exact method show higher amounts. The results of exact-method shown at Figures 34 to 35. The general trend of this method is very similar to CQC and DSC method. In these figures the curves rises linearly and then increases with exponentially trend by some oscillations.

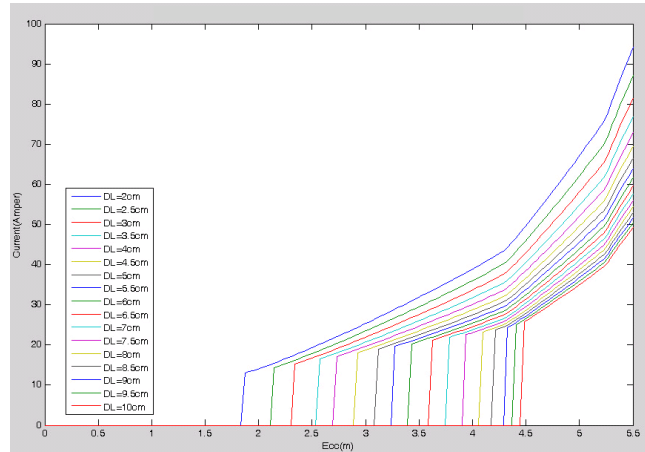


Figure 26. The relation between eccentricity and current in MR damper with DSC method, in x-direction.

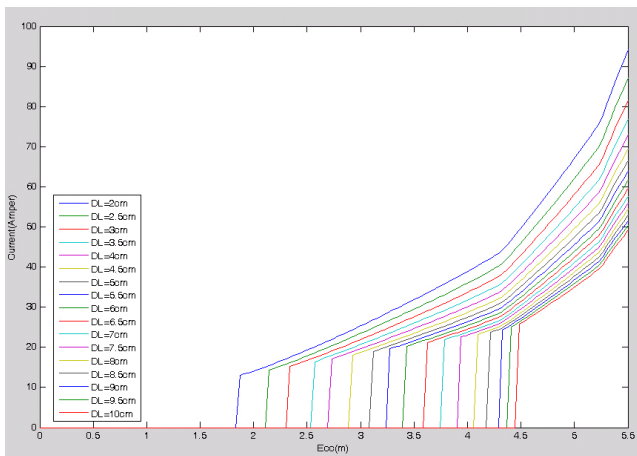


Figure 24. The relation between eccentricity and current in MR damper with CQC method, in x-direction.

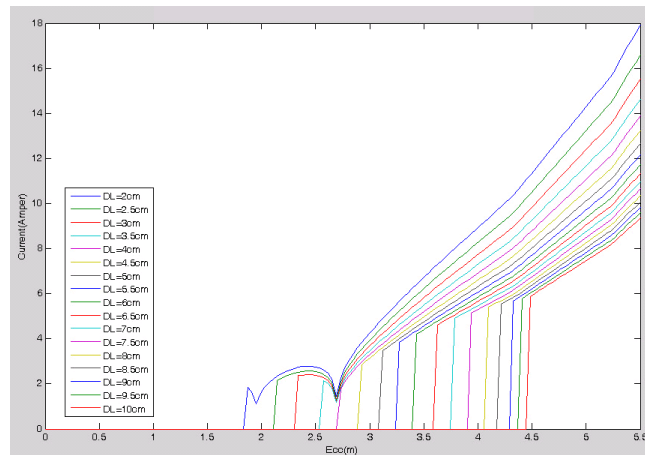


Figure 27. The relation between eccentricity and current in MR damper with DSC method, in y-direction.

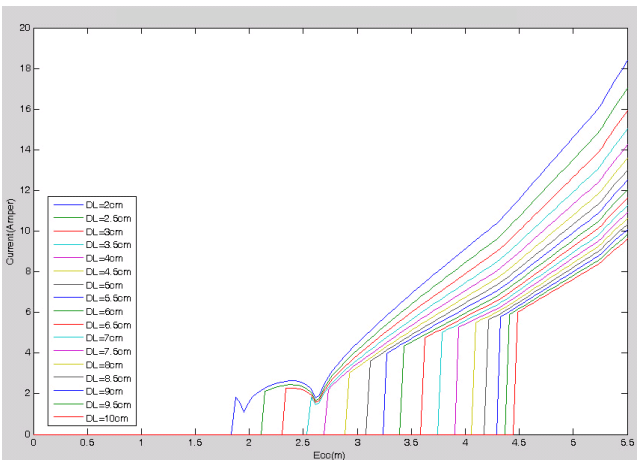


Figure 25. The relation between eccentricity and current in MR damper with CQC method, in y-direction.

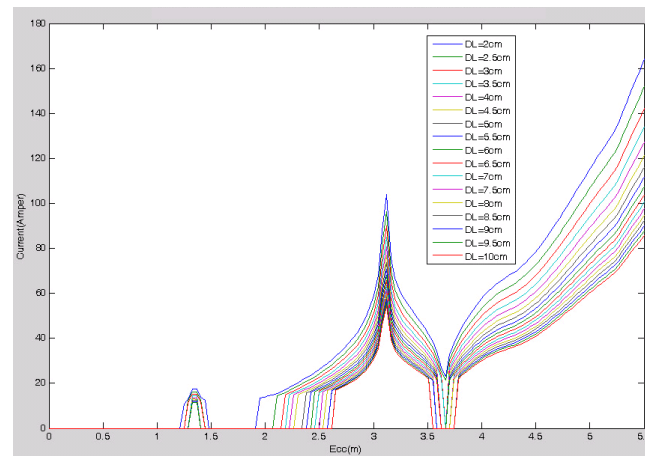


Figure 28. The relation between eccentricity and current in MR damper with Vanmark method, in x-direction.

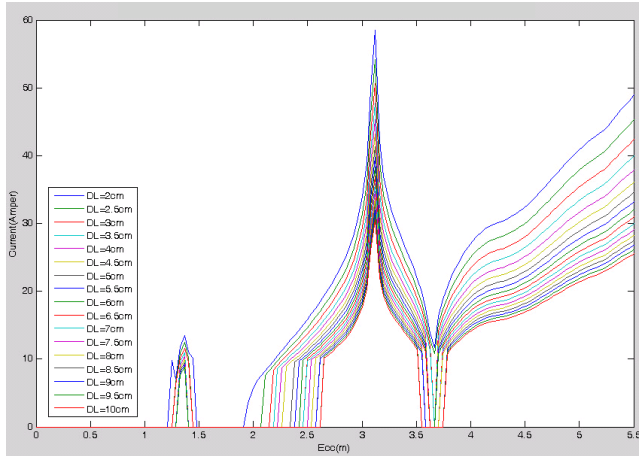


Figure 29. The relation between eccentricity and current in MR damper with Vanmark method, in y-direction.

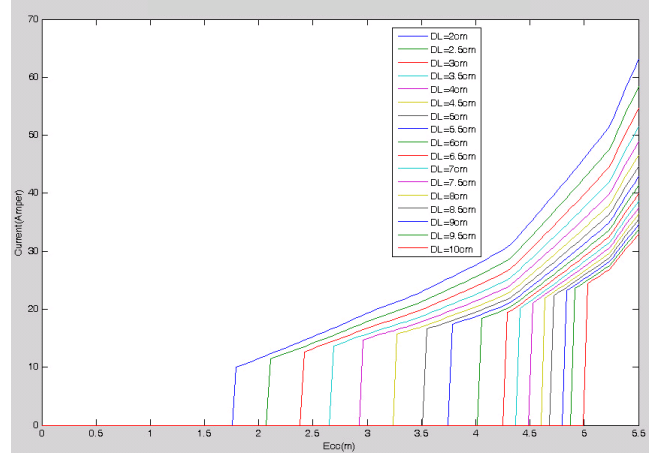


Figure 32. The relation between eccentricity and current in MR damper with Gupta method, in x-direction.

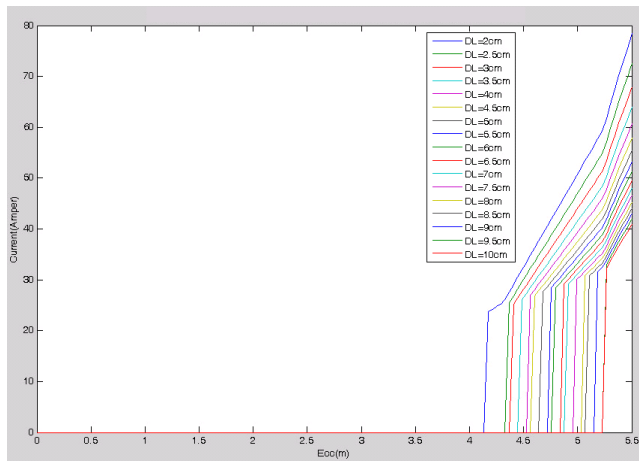


Figure 30. The relation between eccentricity and current in MR damper with Humar method, in x-direction.

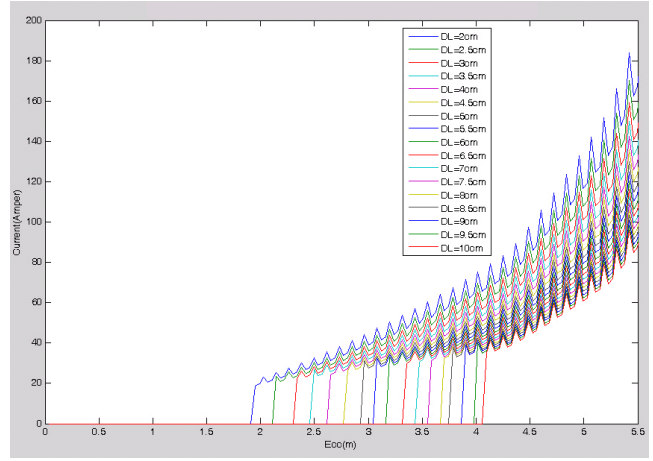


Figure 33. The relation between eccentricity and current in MR damper with Gupta method, in y-direction.

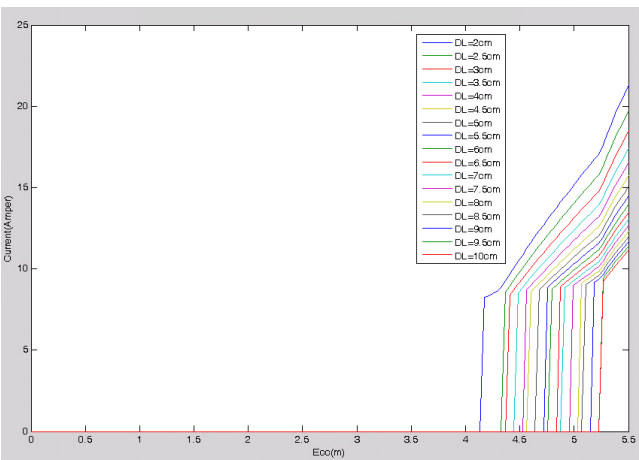


Figure 31. The relation between eccentricity and current in MR damper with Humar method, in y-direction.

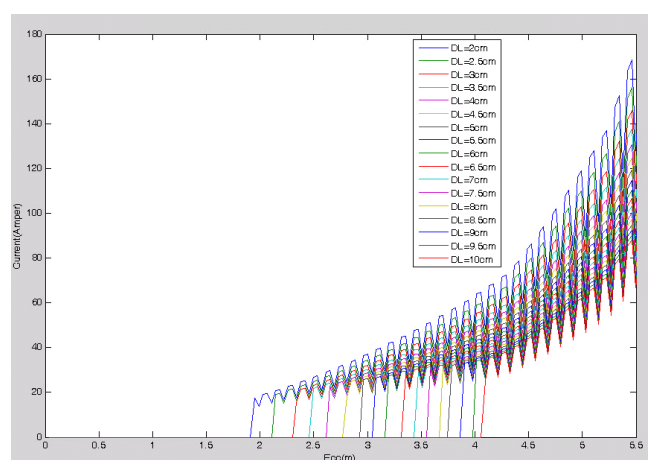


Figure 34. The relation between eccentricity and current in MR damper with exact-method, in x-direction.

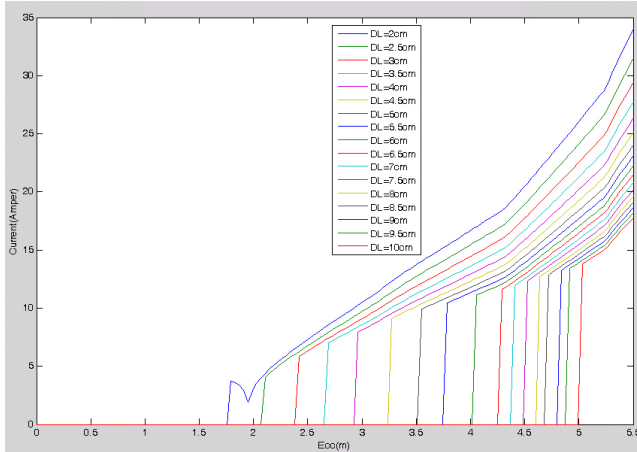


Figure 35. The relation between eccentricity and current in MR damper with exact-method, in y -direction.

6. Conclusion

In this article the torsional behavior due to time-varying eccentricity of load has considered for structure with MR damper as a semi-active control system by the Bingham plasticity model. By changing eccentricity of load in an earthquake due to damages that imposed to structure, the stiffness matrix changes along with earthquake. The corner lateral displacements can be great, so an MR damper used for corner lateral displacement of building. This semi-active system has acceptable performance in transitional and rotational modes, but the main purpose of using this system is to control torsional modes. For controlling the corner lateral displacement due to an earthquake the external braces used, which equipped to MR dampers and photoelectric sensors. This paper shows that by using this system, it is possible to control these displacements by using proper input of current in this system according to target displacement. By reducing the target displacement and increasing eccentricity of load, the resistance forces, shear stresses and input currents in MR damper were increased.

The diagrams show that at lower level of loads and higher target displacement, the MR dampers will not be activated. All of these functions done with photoelectric sensors, which estimate the distance of floor rather than first location. According to target displacement and earthquake loads for any building it's possible to design a proper MR damper for controlling system. This means for any performance base design of structure for example collapse prevention, life safety, immediate occupancy and etc. it is possible to choose a certain target displacement

and according to current-eccentricity diagram, an appropriate MR damper is being designed and the proper algorithm of current was selected. For any power failure, the backup power system must be considered, which needs to be activated during an earthquake. It seems this system can be used for short buildings. The CQC and DSC methods are well adapted to exact-method and can be used for time-varying torsional behavior buildings, but the other methods are not suitable for these kind of buildings.

7. References

1. Spencer BF, Dyke SJ, Sain MK, Carlson JD. Phenomenological model for magnetorheological dampers. *ASCE Journal of Engineering Mechanics*. 1997; 123(3):230–8.
2. Tsang HH, Su KL, Chandler AM. Simplified inverse dynamics models for MR fluid dampers. *Engineering Structures*. 2006; 28(3):327–41.
3. Dyke SJ, Spencer BF, Sain MK, Carlson JD. Modeling and control of magnetorheological dampers for seismic response reduction. *Smart Materials and Structures*. 1996; 5:565–75.
4. Dyke SJ, Spencer BF, Sain MK, Carlson JD. Experimental verification of semi-active control strategies using acceleration feedback. *Proceedings of 3rd International Conference on Motion and Vibration Control*; 1996. 3:291–6.
5. Carlson JD, Spencer BF. Magnetorheological fluid dampers for semi-active control. *Proceedings of the 3rd International Conference on Motion and Vibration Control*; 1996. 3:35–40.
6. Spencer BF, Dyke SJ, Sain MK, Carlson JD. Phenomenological model for magnetorheological dampers. *ASCE Journal of Engineering Mechanics*. 1997; 123(3):230–8.
7. Dyke SJ, Spencer BF Jr, Sain MK, Carlson JD. Seismic response reduction using magnetorheological dampers. *Proceedings of the IFAC World Congress*; San Francisco, CA. 1996 Jun 30-Jul 5.
8. Hosseini M, Legzian Gh. Derivation of stiffness and mass matrices of torsional buildings in fully irregular state. 2011.
9. Ghasemi MR, Barghi E. Estimation of inverse dynamic behavior of MR dampers using artificial and fuzzy-based neural networks. *International Journal of Optimization in Civil Engineering*. 2012; 2(3):357–68.
10. Mousaad A. Vibration control of buildings using magnetorheological damper: A new control algorithm. *Hindawi Publishing Corporation Journal of Engineering*. 2013. Article ID 596078.
11. Dyke SJ, Spencer BF Jr, Sain MK, Carlson JD. An experimental study of MR dampers for seismic protection. *Smart Materials and Structures*. 1998; 7(5):693–703.

12. Spencer BF Jr, Yang G, Carlson JD, Sain MK. Smart dampers for seismic protection of structures: a full-scale study. *Proceedings of the 2nd World Conference on Structural Control*; Kyoto, Japan. 1998; 1:417–26.
13. Yang G, Spencer BF Jr, Carlson JD, Sain MK. Large-scale MR fluid dampers: modeling and dynamic performance considerations. *Engineering Structures*. 2002; 24(3):309–23.
14. Hosseini M, Fanaie N, Yousefi A. Studying the vulnerability of steel moment resistant frames subjected to progressive collapse. *Indian Journal of Science and Technology (INJST)*. 2014; 7(3):335–42.
15. Banihashemi A, Mirzagoltabar A, Tavakoli H. Development seismic design of steel moment frames and the evaluation by energy spectrum method. *Indian Journal of Science and Technology (INJST)*. 2014; 7(10):1699–711.
16. Banihashemi A, Mirzagoltabar A, Tavakoli H. The effects of yield mechanism selection on the performance based plastic design of steel moment frame. *Indian Journal of Science and Technology (INJST)*. 2015; 8(59):157–66.